Journal of Applied Toxicology

WILEY

Journal of AppliedToxicology

RESEARCH ARTICLE

A Novel Regulatory Network of Noncoding RNAs in the Cadmium-Induced Malignant Transformation of Human Bronchial Epithelial Cells

Yueqing Shao[1] | Pengya Zhao[1] | Linlin Wang[2] | Yanfang Yang[1] | Lihua Huang[1,3]

[1]School of Public Health, Baotou Medical College, Baotou, China | [2]The Third Hospital of Baogang Group, Baotou, China | [3]School of Public Health, Shantou University, Shantou, China

Correspondence: Lihua Huang (huanglihua858@163.com; huanglihua@btmc.edu.cn)

Received: 14 March 2025 | **Revised:** 11 April 2025 | **Accepted:** 4 June 2025

Funding: This work was supported by the Special Scientific Research Fund for the Doctoral Program in Public Health and Preventive Medicine of Baotou Medical College (BYJJ-GWZX202505), the National Natural Science Foundation of China (82373624 and 82160630), the Natural Science Foundation of Inner Mongolia (2023LHMS08010), and the Innovation Team of Baotou Medical College (bycxtd-09).

Keywords: 16HBE | cadmium | malignant transformation | noncoding RNAs | regulatory network

ABSTRACT

Long-term exposure to cadmium (Cd) is closely linked to an increased risk of lung cancer, yet the underlying mechanisms driving this malignant transformation remain elusive. Noncoding RNAs may hold the key to understanding the complex pathways involved in cadmium-induced carcinogenesis. This study reveals a novel regulatory network involving circ_000877, lnc237177, and miR-3192-5p, which targets cyclin-D1(CCND1) and matrix metalloproteinase 2 (MMP-2), thereby promoting the Cd-induced malignant transformation of human bronchial epithelial (16HBE) cells. Utilizing an established 16HBE malignant transformation model induced by Cd exposure, RNA sequencing and quantitative real-time polymerase chain reaction (qRT-PCR) analyses indicated that both circ_000877 and lnc237177 were significantly upregulated. Functional assays further confirmed the roles of these molecules in facilitating malignant transformation. Mechanistically, circ_000877 and lnc237177 collaboratively targeted miR-3192-5p, thereby modulating both mRNA and protein expression levels of cyclin-D1 and MMP-2. Collectively, this study offers novel perspectives into the mechanism through which circRNA and lncRNA jointly regulate miRNA in a crosstalk network during Cd-induced malignant transformation, thereby enhancing our understanding of cadmium's toxicological impact.

1 | Introduction

Cadmium (Cd), a prevalent heavy metal environmental contaminant, exhibits significant biological toxicity, characterized by teratogenic, carcinogenic, and mutagenic properties. Chronic exposure to Cd can result in severe damage to vital organs, including the kidneys and liver, especially the lungs (Liu et al. 2023). Cd primarily enters the human body via inhalation, with fine particulate matter or vapors accumulating in the lungs and subsequently dispersing systemically. Increasing evidence demonstrates that Cd exposure is associated with respiratory disorders such as pulmonary edema, pulmonary fibrosis, and lung cancer. Epidemiological research involving 336 lung cancer patients utilized Cox proportional hazard analysis to examine the correlation between blood Cd concentrations and overall survival, indicating that lower blood Cd levels might predict improved survival outcomes in patients with early-stage lung cancer (Pietrzak et al. 2021). Jiang et al. (2021) further confirmed in a cohort of 860 cancer patients that chronic low-dose Cd exposure was positively correlated with elevated mortality rates

Yueqing Shao, Pengya Zhao and Linlin Wang contributed equally to this work.

across various cancer types, including lung cancer. A recent study investigating the association between blood concentrations of heavy metals and the risk of site-specific cancer mortality among cancer survivors revealed that elevated whole-blood cadmium levels were positively correlated with both all-cause mortality and cancer-specific mortality in this population (Yan et al. 2025). McGraw et al. (2024) analyzed data from 6418 MESA subjects and found that exposure to cadmium was associated with the degree of coronary artery calcification. Due to its high toxicity, the European Union classifies Cd as a hazardous carcinogenic substance and strictly regulates its use. Despite increasing public health concerns regarding Cd exposure, existing studies predominantly address liver dysfunction, nephrotoxicity, and reproductive disorders, with relatively limited attention devoted to pulmonary diseases. Consequently, further investigation into the specific molecular mechanisms underlying Cd-induced lung carcinogenesis is urgently needed.

Recently, the relationship between noncoding RNAs and cancer pathogenesis has attracted considerable scientific interest. Extensive studies on circular RNAs (circRNAs)/long noncoding RNAs (lncRNAs) have highlighted their active participation in disease progression through complex interactions with microRNA (miRNA) molecules (Cui et al. 2023; Liu et al. 2022; Hu et al. 2022). Emerging evidence indicates circRNAs, lncRNAs, and miRNAs form intricate regulatory networks capable of modulating cancer initiation, progression, and therapeutic outcomes. For instance, circRNA104250 and lncRNAuc001.dpp.1 have been reported to target miR-3607-5p, thereby influencing interleukin-1 receptor 1 (IL1R1) expression and subsequently affecting the nuclear factor kappa B (NF-κB) signaling pathway (Li, Jia, et al. 2019). Another study established a circRNA-lncRNA-miRNA-mRNA competitive endogenous RNA (ceRNA) network implicated in hepatocellular carcinoma (HCC) prognosis, demonstrating that deletion of DTYMK suppressed HCC cell proliferation and invasion, providing comprehensive insights into ceRNA mechanisms involved in HCC pathogenesis (Zhang et al. 2021). Nevertheless, research on the functional impacts of Cd exposure on noncoding RNAs and related regulatory networks remains limited. Therefore, deeper exploration of the competitive cobinding of miRNAs by circRNAs and lncRNAs in Cd-induced disease processes is essential.

In the present study, we delineated a novel regulatory network consisting of circ_000877 and lnc237177 cotargeting miR-3192-5p, elucidating their role in the carcinogenic transformation of human bronchial epithelial (16HBE) cells induced by Cd. This research offers valuable new insights into noncoding RNA regulatory networks and significantly advances our understanding of the related molecular mechanisms associated with Cd-induced malignancies in human lung cells.

2 | Materials and Methods

2.1 | Cellular Culture

The human bronchial epithelial cell line (16HBE) was generously provided by the Institute of Chemical Carcinogenesis at Guangzhou Medical University (Guangzhou, China). Cells were cultured in basal medium (pH = 7.2), specifically Minimum Essential Medium (MEM; Geno Company, Hangzhou, China), enriched with 10% fetal bovine serum (Sijiqing Company, Hangzhou, China) and 1% penicillin–streptomycin mixture (Gibco, Gaithersburg, United States). Cultures were maintained in an incubator at 37°C under an atmosphere containing 5% CO_2. Cadmium chloride (Sigma Corporation, United States) was prepared by dissolving 18.3-mg powder in 1 mL of sterile phosphate-buffered saline (PBS). Subsequently, serial dilutions were performed to achieve a final concentration of 2 μmol/L in the culture medium. Cells cultured in standard medium served as the control group, whereas cells exposed to medium supplemented with cadmium chloride constituted the experimental group. Both groups were cultured continuously for 40 weeks, with routine passaging performed twice weekly.

2.2 | Selection of Exposure Concentration

Based on the calculation method described in the literature (Wang et al. 2024), the lowest exposure dose was selected to estimate the annual cumulative inhaled cadmium (Cd) quantity, calculated as approximately 0.25 μg × 10 cigarettes per day × 365 days, yielding 912.5 μg/year. Considering the molar mass of Cd to be 112 g/mol, the total concentration for cellular exposure was calculated by dividing 912.5 μg by a lung fluid volume that varies between 2000 and 5000 mL. This yielded a concentration range of 182.5–456.25 μg/L, which corresponds to 1.63–4.07 μM. Therefore, a minimum cumulative exposure concentration of 2 μM was selected for the experimental exposure of 16HBE cells.

2.3 | Wound Healing Test

The cells were seeded onto a six-well culture plate, and after the growth confluence reached 100%, the cells were scratched vertically with a 200-μL pipette tip, rinsed with PBS three times, added the growth medium without fetal bovine serum and antibiotics, and photographed and recorded the scratch area under the microscope. After being cultured in the 37°C/5% CO_2 incubator for 24 h, the scratch area was recorded in the same position, and the percentage of scratch healing area was evaluated using ImageJ software (Version 1.54 g).

2.4 | Colony-Formation Assay

To conduct the colony-formation assay, 16HBE cells were seeded into six-well plates at a density of 100 cells per well and cultured continuously until visible colonies emerged. The number of colonies formed in each well was documented and compared between groups. Following fixation, the colonies were stained using crystal violet and subsequently incubated for a 20-min period. Subsequently, the wells were photographed, and colonies visible to the naked eye were counted. The clone formation rate was calculated as follows: (number of colony-forming cells / number of inoculated cells) × 100%.

A base layer was prepared by adding 2 mL of 1.2% low-melting-point agarose (dissolved in 2× MEM) to each well of a six-well plate, followed by solidification at room temperature.

Subsequently, mix 0.5 mL of 16HBE cell suspension (100 cells per well) with an equal volume of 0.6% low-gelling-temperature agarose. Overlay the mixture onto the solidified base layer in the wells. Cultivate the plates in an incubator with 5% CO_2 at 37°C for 14–21 days. After cultivation, count and image the colonies under an optical microscope.

2.5 | RNA Sequencing

After total RNA extraction from the normal 16HBE cells and malignant transformed 16HBE cells exposed to Cd for 30 weeks, ribosomal RNA was removed. The mRNA is subsequently enriched using magnetic beads and fragmented through high-temperature treatment. The fragmented mRNA serves as a template in various reverse transcriptase reaction systems for cDNA synthesis. The purified cDNA is then amplified via PCR, and the completed sequencing library is sequenced using the Illumina NovaSeq X Plus PE150 mode.

2.6 | RNA Isolation and Quantitative Real-Time Polymerase Chain Reaction (qRT-PCR)

Total RNA was isolated and purified using TRIzol UP reagent (Invitrogen Corporation, United States) according to the manufacturer's instructions. CircRNA and lncRNA cDNA were synthesized using standard reverse transcription kits (Promega Corporation, United States), whereas miRNA was converted to cDNA using a miRNA-specific reverse transcription kit (Epicentre miRNA First-Strand cDNA Synthesis Kit, Madison, WI). Quantitative real-time PCR (qRT-PCR) analysis was performed using SYBR Green PCR Master Mix (Promega Corporation, United States) to quantify RNA expression levels. Relative gene expression was adjusted to internal reference genes (GAPDH or U6) and quantified using the 2^−ΔΔCt method. The qRT-PCR primers were meticulously crafted using Primer-BLAST (https://www.ncbi.nlm.nih.gov/tools/primer-blast/), ensuring their unparalleled specificity through rigorous computational validation. The sequence is shown in Table S1.

2.7 | Localization in the Cytoplasm and Nucleus

Cytoplasmic and nuclear fractions of RNA from 16HBE cells were extracted using the PARIS kit (Ambion, Austin, TX, United States), following the manufacturer's protocol precisely. Subsequently, RNA extracted from these fractions was reverse-transcribed into complementary DNA (cDNA), and gene expression levels were quantified using qRT-PCR. U6 and GAPDH were designated as the reference genes for the nuclear and cytoplasmic fractions, respectively, showcasing their pivotal roles in gene expression analysis.

2.8 | Delinearized Enzyme Experiment

Cellular RNA was extracted and quantified. Subsequently, three units of RNase R enzyme were added per 1000 ng of RNA, with the buffer volume adjusted according to the following formula: (RNA volume + RNase R volume) / 10. After thorough mixing, the reaction mixture was incubated at 37°C for 10 min, followed by reverse transcription into cDNA.

2.9 | Immunofluorescence Assay

16HBE cells were seeded onto coverslips. Once cells reached approximately 70% confluence, they were fixed using prechilled 4% paraformaldehyde at 4°C for 20 min. Subsequently, cells were incubated overnight at 4°C with primary antibodies against Matrix Metalloproteinase-2 (MMP-2; dilution 1:500; Bioss, Beijing, China) and Cyclin-D1 (CCND1; 1:50; Bioss, Beijing, China). After incubation, the cells were washed and then incubated at room temperature for 2 h with an Alexa Fluor 488-conjugated goat antirabbit secondary antibody (IgG; Invitrogen, United States), which was diluted in phosphate-buffered saline (PBS) supplemented with 0.2% bovine serum albumin (BSA). The nuclei were stained with 4′,6-diamidino-2-phenylindole (DAPI, 60 μL per well) for a duration of 5–10 min at room temperature. Fluorescent images were captured by confocal microscopy (Nikon, Japan), maintaining consistent parameters (e.g., exposure time and gain settings) across all samples for comparative analyses.

2.10 | Cell Transfection

Transfection of miRNA mimics and inhibitors was performed using Ribo FECT CP reagent (RiboBio, Guangzhou, China), whereas plasmid DNA transfections utilized Lipofectamine 2000 reagent (Thermo Fisher Scientific, United States), strictly adhering to the manufacturers' protocols. Cells were transfected upon reaching approximately 70% confluence. Six hours after transfection, the culture medium was refreshed with a new one. The specific sequences of miRNA mimics and inhibitors utilized in this study are provided in Table S2.

2.11 | Dual Luciferase Reporter Gene Assay

Dual luciferase reporter vectors carrying either wild-type or mutated binding sites of circ_000877 and lnc237177 were constructed based on predicted miR-3192-5p binding regions. Subsequently, the vectors were jointly introduced into 293-T cells together with either miR-3192-5p mimics or the corresponding negative controls (NC). After 24 h of incubation, luciferase activity was measured utilizing the Dual-Luciferase Reporter Assay System (Promega, United States). An enzyme-labeling instrument was employed to detect firefly luciferase activity at 560 nm and Renilla luciferase activity at 460 nm. The relative luciferase activity was determined by calculating the ratio of firefly luciferase output to Renilla luciferase output, thereby providing a normalized measure of expression efficiency.

2.12 | Statistical Analysis

All experiments were independently performed in triplicate. Data were expressed as mean ± standard deviation (SD).

Statistical analyses were conducted using SPSS 22.0 software (IBM, Armonk, NY, United States) and GraphPad Prism v8.0 (GraphPad, San Diego, CA, United States). The comparisons between two groups were evaluated using Student's two-tailed *t* tests, and statistical significance was set at $p < 0.05$.

3 | Results

3.1 | Cd Triggered Malignant Transformation in 16HBE Cells

Based on the calculated concentration of Cd exposure, we chose 2-μM Cd to treat 16HBE cells for 40 weeks to establish a malignant transformation model (named 16HBE-T). The 16HBE-T cells were appraised via the scratch assay and colony-formation assay. The results of the wound healing assays revealed significantly accelerated cell migration in the 16HBE-T relative to control cells (Figure 1A). Similarly, colony-formation assays showed that the colony count significantly increased in the 16HBE-T cells compared to the control group (Figure 1B,C). Quantitative real-time PCR (qRT-PCR) analysis indicated markedly elevated mRNA expression levels of CCND1 and MMP-2 in 16HBE-T cells compared to controls (Figure 1D). Furthermore, immunofluorescence assays demonstrated enhanced average fluorescence intensities of CCND1 and MMP-2 proteins in the 16HBE-T cells relative to the control group (Figure 1E). Collectively, these findings reveal that prolonged exposure to Cd profoundly accelerates the malignant transformation of 16HBE cells.

3.2 | The Expression Levels and Functions of circ_000877 and lnc237177

We submitted normal 16HBE and 16HBE-T cells to biotechnology companies for RNA sequencing to screen differentially expressed circRNA and lncRNA (> 2.0-fold change) (Figure S1). qRT-PCR validation confirmed that circ_000877 and ENST000237177 (lnc237177) were the most significantly upregulated in 16HBE-T cells (Figure 2A,B). Bioinformatics analysis using circBase (http://www.circbank.cn/) revealed that circ_000877 is located on chromosome 16, spans 891 bp, and originates from ACSF3 (Figure 2C). Meanwhile, lnc237177 is located on chromosome 6 and comprises 10 exons spanning 44,557 bp. After RNase R treatment in 16HBE-T cells, the expression of linear GAPDH and the parental ACSF3 was significantly reduced. In contrast, the expression of circ_000877 remained unchanged, indicating that circ_000877 possesses a highly stable circular structure (Figure 2D).

To assess their function, we transfected 16HBE-T cells with siRNA targeting circ_000877 or lnc237177. Knockdown efficiencies were 82.2% and 73.2% for circ_000877 (Figure 2E) and 63.4% and 75.6% for lnc237177 (Figure 2F). Notably, circ_000877 knockdown did not affect ACSF3 expression (Figure 2G). Functional assays showed that silencing circ_000877 or lnc237177 significantly reduced cell migration (Figure 2H). qRT-PCR revealed decreased CCND1 and MMP-2 mRNA levels following their knockdown (Figure 2I,J), with a greater reduction observed upon simultaneous knockdown. Immunofluorescence

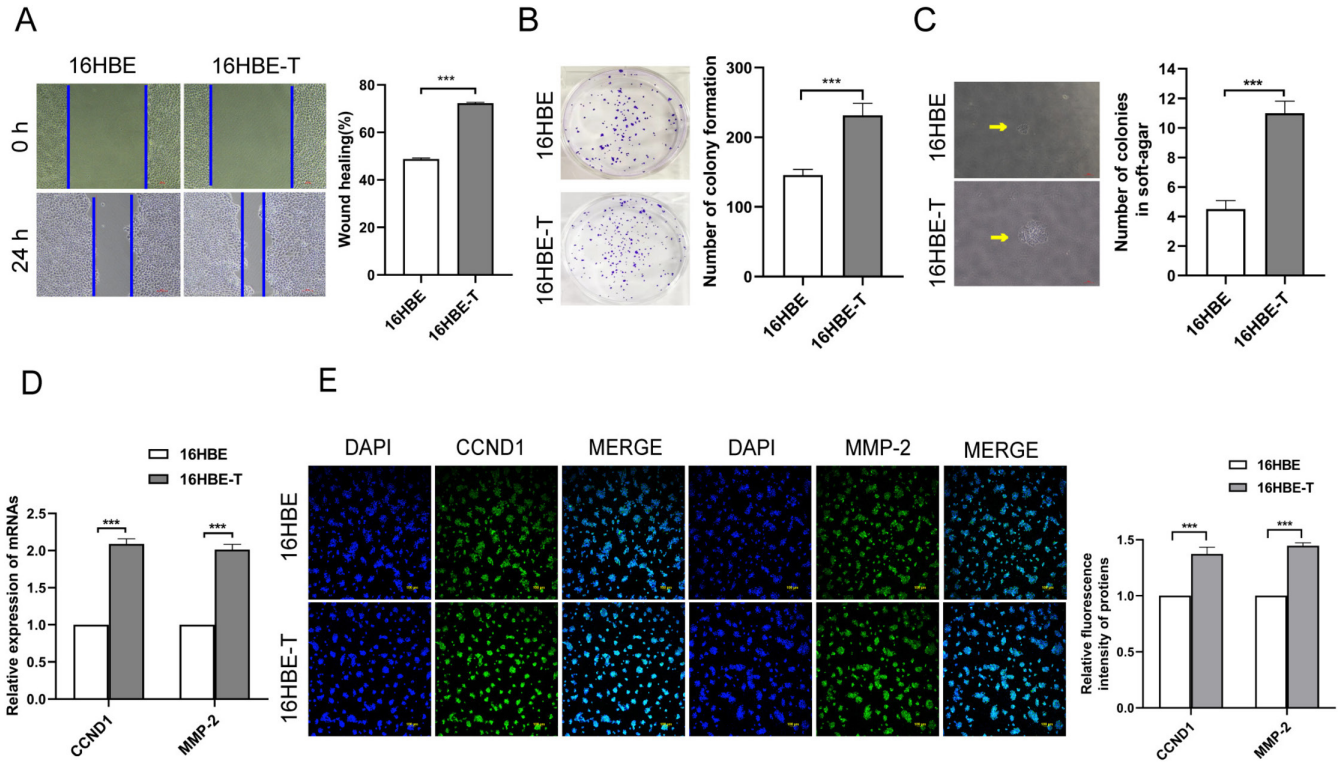

FIGURE 1 | Cd triggered malignant transformation within 16HBE cells. (A) Wound healing assay was used to detect the migration ability of cells in the exposed group and the control group. (B) The proliferation ability of cells in the exposed group and the control group was detected by colony survival assay. (C) Colony formation test showed that the anchoring of cells in the exposed group and the control group was independent. (D) qRT-PCR was used to detect the expression of CCND1 and MMP-2 in the exposed group and control group. (E) Protein immunofluorescence assay was used to detect the expression of CCND1 and MMP-2 in the exposed group and the control group. Data are shown as means ± SD, $n = 3$. $^{***}p < 0.001$.

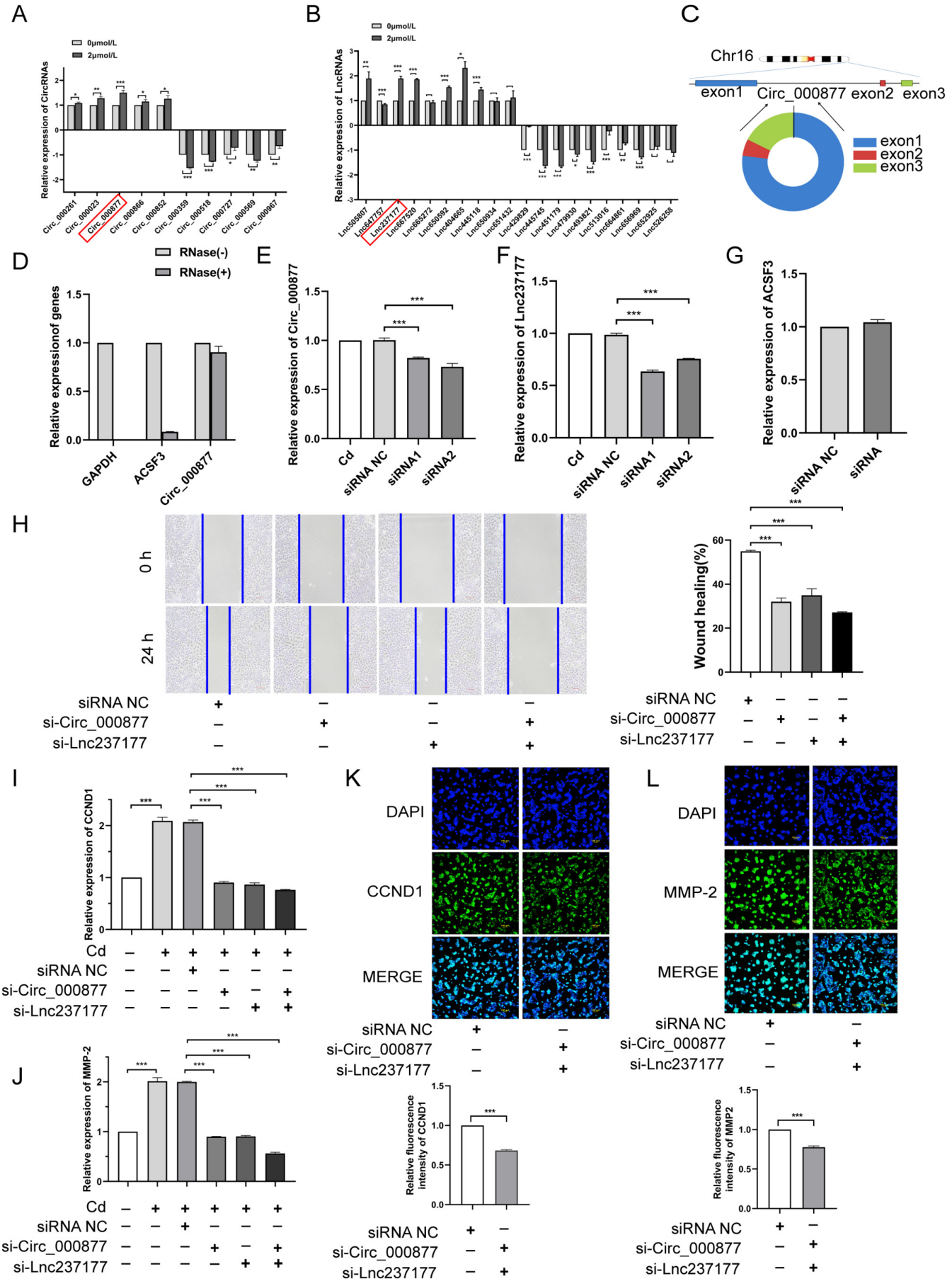

FIGURE 2 | Legend on next page.

FIGURE 2 | The expression levels and functions of circ_000877 and lnc237177. (A, B) qRT-PCR results of circRNAs showed that circ_000877 and lnc237177 were significantly increased. (C) The genomic location and loop diagram of circ_000877. (D) The expression of GAPDH, ACSF3, and circ_000877 in RNAs treated with or without RNase R was detected by q-PCR. (E, F) The interference efficiency of circ_000877 and lnc237177 were detected by qRT-PCR. (G) The expression level of ACSF3 of circ_000877 parent gene was detected by qRT-PCR. (H) Wound healing assay was used to detect cell migration after interference with circ_000877 and lnc237177. (I, J) The expression levels of CCND1 and MMP-2 were detected by qRT-PCR after interference with circ_000877 and lnc237177. (K, L) The expression levels of CCND1 and MMP-2 were detected by immunofluorescence assay after interference of circ_000877 and lnc237177. Data are shown as means ± SD, $n = 3$. $_{*}p < 0.05$, $_{**}p < 0.01$, $_{***}p < 0.001$.

confirmed a significant decline in CCND1 and MMP-2 protein expression (Figure 2K,L). These findings suggest that circ_000877 and lnc237177 promote Cd-induced malignant transformation by regulating CCND1 and MMP-2 expression.

3.3 | circ_000877 and lnc237177 Jointly Target miR-3192-5p and Regulate Its Expression

Using cytoplasmic-nuclear fractionation assays, we examined the cellular localization of circ_000877 and lnc237177, employing GAPDH as a cytoplasmic marker and U6 as the intracytonuclear reference. The results indicated that both circ_000877 and lnc237177 were mainly expressed in the cytoplasm (Figure 3A,B). Bioinformatics analysis using TargetScan (https://www.targetscan.org/vert_80/) identified 14 candidate miRNAs predicted to interact with circ_000877 and lnc237177. Among these, four miRNAs implicated in tumorigenesis were selected for expression analysis (Figure 3C). qRT-PCR demonstrated that these four miRNAs exhibited significantly decreased expression in 16HBE-T cells compared with the control group (Figure 3D). After individual or combined knockdown of circ_000877 and lnc237177 using small interfering RNA (siRNA), the expression levels of these miRNAs were significantly increased compared to negative controls, with combined knockdown producing a more pronounced elevation (Figure 3E–H). These results suggested that circ_000877 and lnc237177 can negatively regulate the expression of 4 miRNAs in16HBE-T cells.

Further analysis utilizing the starBase database (http://starbase.sysu.edu.cn/) predicted binding sequences between miR-3192-5p and both circ_000877 and lnc237177 (Figure 3I). The results of the dual-luciferase reporter gene assay indicated that the firefly luciferase activity, cotransfected with WT-circ_000877/WT-lnc237177 and miR-3192-5p mimics, was significantly reduced compared to the control group (Figure 3J,K). These findings confirm that circ_000877 and lnc237177 directly bind miR-3192-5p, negatively regulating its expression in Cd-induced malignant transformation.

3.4 | MiR-3192-5p Inhibited the Malignant Transformation of 16HBE Cells Elicited by Cd

To assess the functional significance of miR-3192-5p, both miRNA mimics and inhibitors were introduced into 16HBE-T cells, with the transfection efficiency evaluated through qRT-PCR analysis. Results confirmed that miR-3192-5p mimics markedly increased miR-3192-5p expression, whereas inhibitors significantly decreased its expression (Figure 4A). However, neither mimics nor inhibitors significantly affected the expression levels of circ_000877 and lnc237177 (Figure 4B). Scratch wound healing assays revealed that transfection with miR-3192-5p mimics significantly reduced cell migration compared with control cells, whereas inhibitors promoted migration (Figure 4C). Consistently, qRT-PCR analysis revealed the mRNA expression levels of CCND1 and MMP-2 were significantly markedly reduced upon miR-3192-5p mimic transfection and increased following inhibitor treatment (Figure 4D). Immunofluorescence assays further confirmed the inhibitory effects of miR-3192-5p mimics on CCND1 and MMP-2 protein expression, whereas inhibitors showed opposite trends (Figure 4E). Collectively, these data suggest that miR-3192-5p exerts inhibitory effects on the Cd-induced malignant transformation of 16HBE cells.

3.5 | Circ_000877 and lnc237177 Cotarget miR-3192-5p to Inhibit Cd-Induced Malignant Transformation of 16HBE Cells

To investigate the role of noncoding RNA networks in Cd-induced malignant transformation of 16HBE cells, we conducted cotransfection with si-circ_000877, si-lnc237177, and a miR-3192-5p inhibitor. Scratch assays showed that the miR-3192-5p inhibitor partially restored cell migration, suppressed by the simultaneous knockdown of circ_000877 and lnc237177 (Figure 5A). qRT-PCR and immunofluorescence confirmed that the miR-3192-5p inhibitor reversed the downregulation of CCND1 and MMP-2 mRNA and protein levels caused by simultaneous knockdown of circ_000877 and lnc237177 (Figure 5B,C). These findings suggest that the miR-3192-5p inhibitor counteracts the tumor-suppressive effects of circ_000877 and lnc237177 knockdown, promoting Cd-induced malignant transformation.

4 | Discussion

This study aimed to clarify the role and molecular pathways of a newly discovered regulatory network comprising circ_000877 and lnc237177. These elements collaboratively target miR-3192-5p, thereby influencing cadmium (Cd)-induced malignant transformation in 16HBE cells. An increasing number of studies highlight the significance of circRNA/lncRNA-miRNA interactions in tumor progression. For instance, recent research by Zhu et al. (2024) revealed that circRNA-lncRNA-miRNA networks serve as essential regulators and potential biomarkers for lung adenocarcinoma (LUAD). Following prolonged Cd exposure, we confirmed malignant transformation in 16HBE cells through wound healing assays and colony-formation assays. Chronic exposure to Cd significantly enhanced the migratory and proliferative capacities of 16HBE cells.

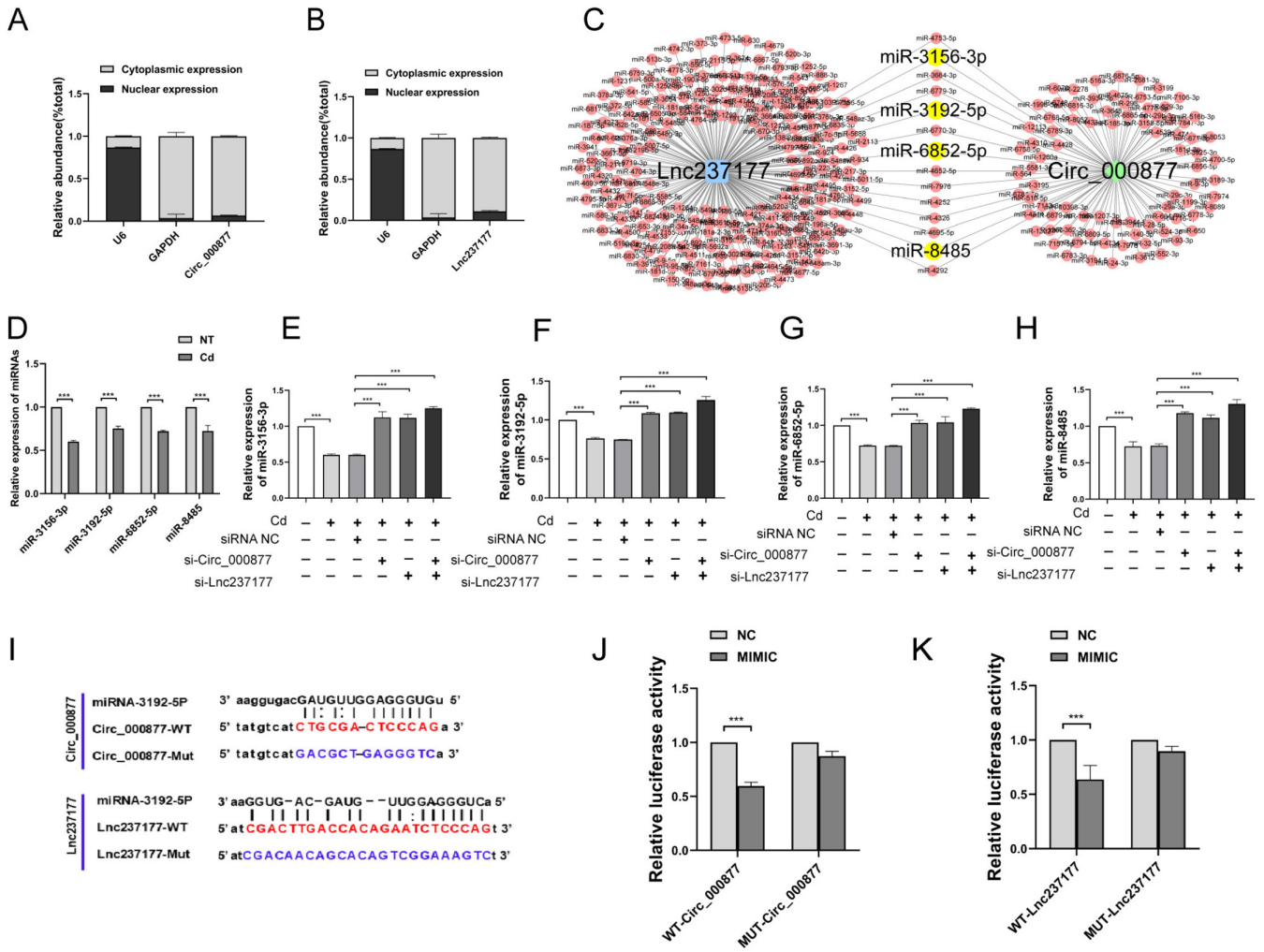

FIGURE 3 | miR-3192-5p effectively inhibited the malignant transformation of 16HBE cells elicited by Cd. (A) The localization of nuclear or cytoplasm of circ_000877 was detected by qRT-PCR. (B) The localization of nuclear or cytoplasm of lnc237177 was detected by qRT-PCR. (C) Prediction of miRNAs cobinding with circ_000877 and lnc237177 by biogenic analysis. (D) Four miRNAs cobound with circ_000877 and lnc237177 were screened, and their expression levels were detected by q-PCR in the malignant transformation cell model. (E–H) The expression of miR-3156-3p, miR-3192-5p, miR-6852-5p, and miR-8485 interfered with circ_000877 and lnc237177 was detected by qRT-PCR. (I) The binding sites of circ_000877 and lnc237177 with miR-3192-5p were predicted. (J, K) Dual luciferase reporter genes verified circ_000877 and lnc237177 binding to miR-3192-5p. Data are presented as means ± SD, $n = 3$. $^{***}p < 0.001$.

Matrix Metalloproteinase 2 (MMP-2) and Cyclin D1 (CCND1) are well-established markers of malignant transformation. CCND1 and MMP-2 play a key role in tumorigenesis and progression. The expression level of MMP-2 is significantly positively correlated with tumor stage and invasion depth, which can reflect the invasion potential of tumors (Kwon et al. 2021; Sun et al. 2023). CCND1, a recognized proto-oncogene, was previously reported to promote tumor progression through circRNA-mediated regulatory networks. Its overexpression or abnormal activation is involved in the progression of various malignant tumors (Valla et al. 2022). Both CCND1 and MMP-2 are widely regarded as important molecular markers of malignant transformation. Our findings indicated that prolonged low-dose Cd exposure significantly upregulated both the mRNA and protein expression of CCND1 and MMP-2 in 16HBE cells, further supporting Cd-induced cellular malignant transformation.

A substantial body of evidence has demonstrated the pivotal roles played by noncoding RNAs in malignant tumors (Wang et al. 2023; Lu et al. 2017). RNA sequencing analyses in our study revealed significant upregulation of circ_000877 and lnc237177 in Cd-induced malignant 16HBE cells. Using RNA interference approaches targeting circ_000877 and lnc237177, we observed that silencing these molecules inhibited the proliferative capability and reduced CCND1 and MMP-2 expression at both mRNA and protein levels in transformed cells.

CircRNAs and lncRNAs control gene expression by acting as competitive endogenous RNAs (ceRNAs), which bind to microRNAs (miRNAs) in a competitive manner, thereby regulating the expression of downstream mRNA targets. Such regulatory interactions, widely reported in the literature, critically influence signaling pathways associated with disease progression (Yao et al. 2022; Chen et al. 2022). Our investigation, guided by

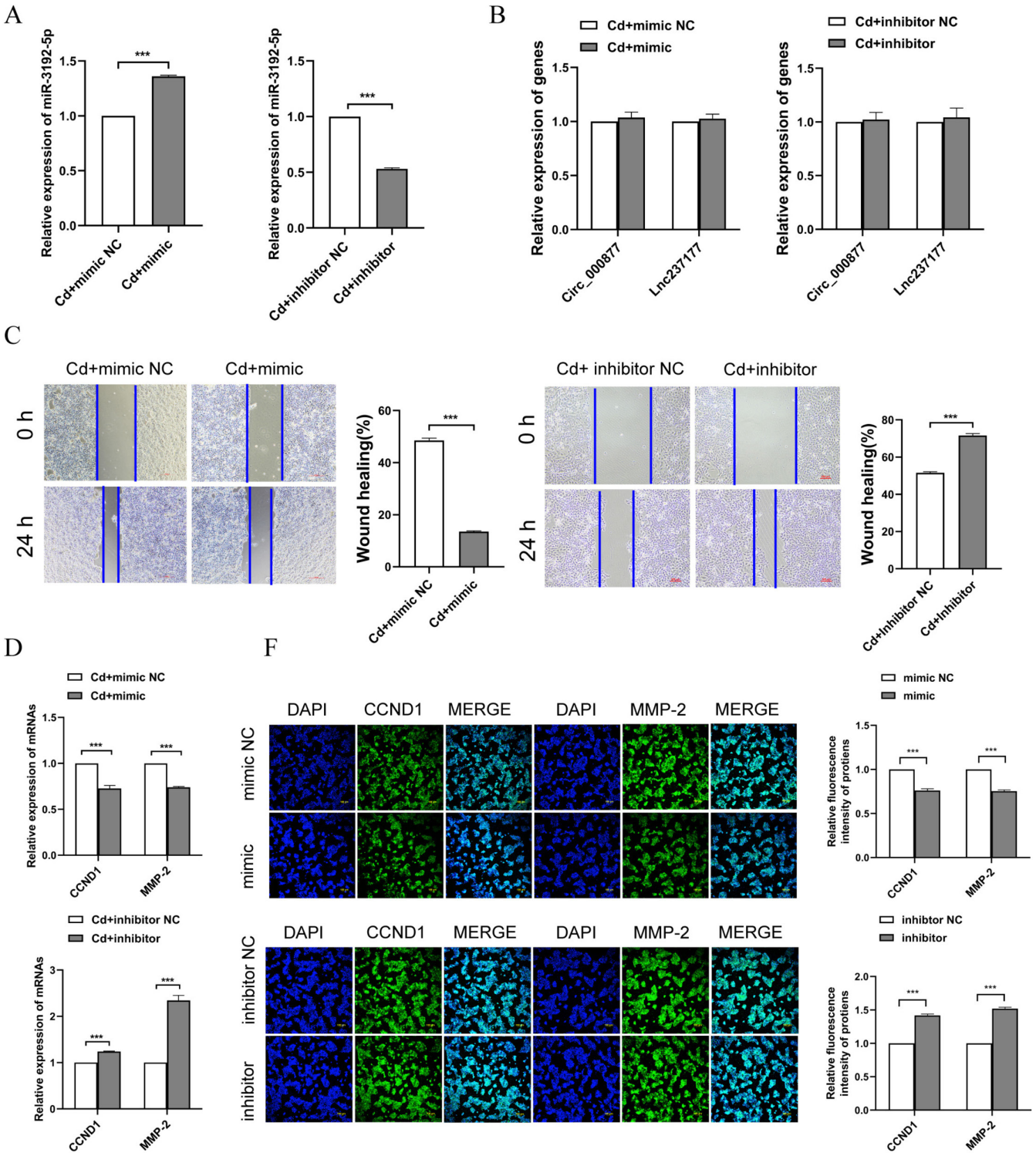

FIGURE 4 | miR-3192-5p effectively inhibited the malignant transformation of 16HBE cells elicited by Cd. (A) The transfection efficiency of miR-3192-5p mimic and inhibitor was determined by qRT-PCR. (B) qRT-PCR was used to detect the expression of circ_000877 and lnc237177 after transfection with miR-3192-5p mimic and inhibitor. (C) Cell migration after transfection with miR-3192-5p mimics and inhibitors was determined by wound healing assay. (D) The expression of the marker proteins CCND1 and MMP-2 after transfection of miR-3192-5p mimic and inhibitor by qRT-PCR. (E) The expression of marker proteins CCND1 and MMP-2 after transfection with miR-3192-5p mimic and inhibitor was detected by protein immunofluorescence. Data are presented as means ± SD, $n = 3$. $^{***}p < 0.001$.

bioinformatics predictions (TargetScan) and validated through dual-luciferase reporter assays, demonstrated direct binding interactions between miR-3192-5p and both circ_000877 and lnc237177. Notably, circ_000877 and lnc237177 negatively regulated miR-3192-5p expression, supporting their involvement as competing endogenous RNAs (ceRNAs). Consistent with prior findings (Li, Wang, et al. 2019), these interactions illustrate the significance of circRNA-lncRNA-miRNA regulatory networks

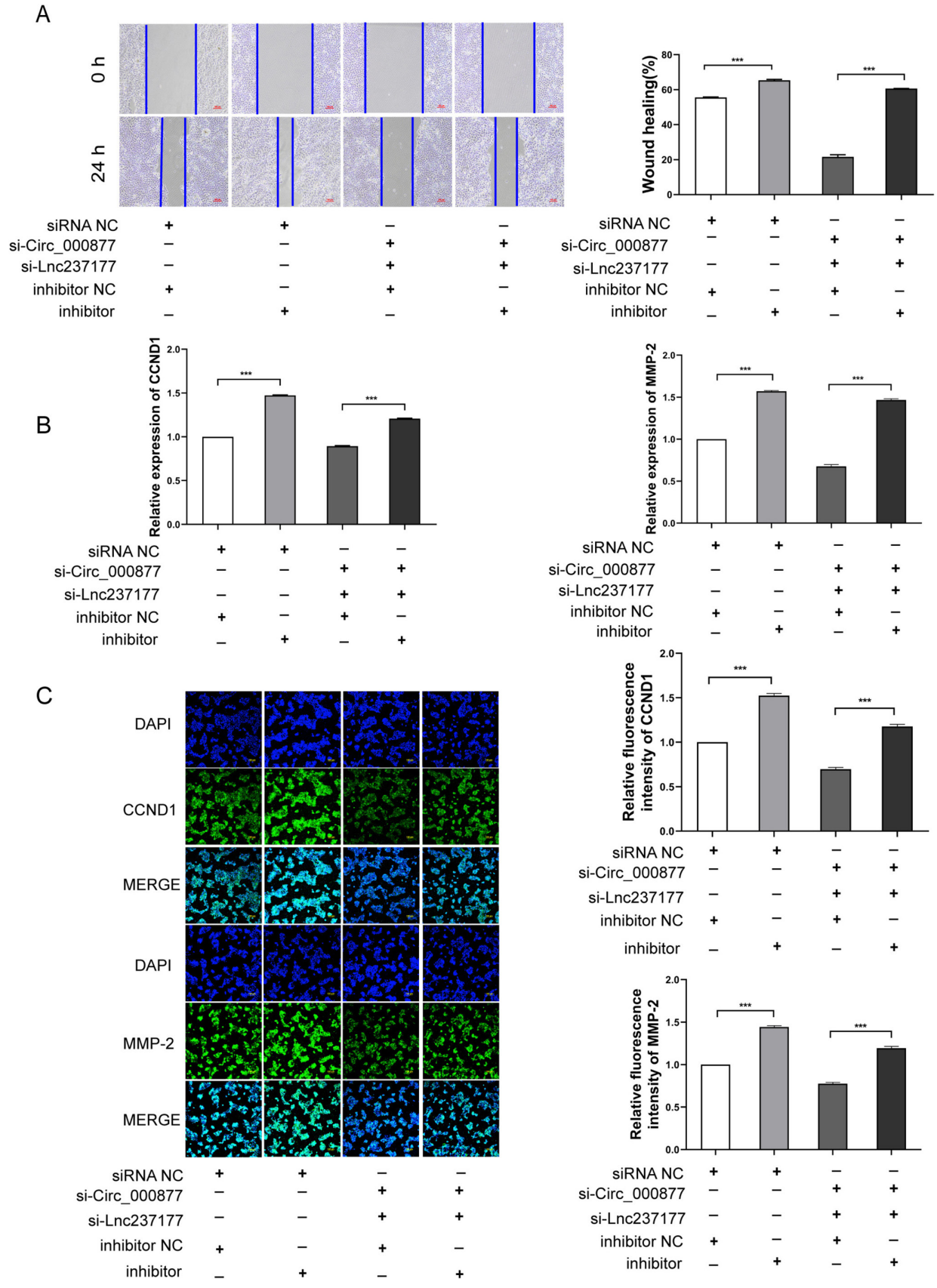

FIGURE 5 | circ_000877 and lnc237177 cotarget miR-3192-5p to inhibit Cd-induced malignant transformation of 16HBE cells. (A) Wound healing assay to detect the ability of cell migration after cotransfection with si-circ_000877 and si-lnc237177 and miR-3192-5p inhibitor. (B) qRT-PCR was used to detect the expression of CCND1 and MMP-2 after cotransfection with si-circ_000877 and si-lnc237177 and miR-3192-5p inhibitor. (C) The expression of CCND1 and MMP-2 was detected by protein immunofluorescence after cotransfection with si-circ_000877 and si-lnc237177 and miR-3192-5p inhibitor. Data are presented as means ± SD, $n = 3$. $^{***}p < 0.001$.

in cellular transformation and carcinogenesis. Moreover, miR-3192-5p was confirmed to play a critical suppressive role in Cd-induced malignant transformation, indicating that this regulatory axis is central to the oncogenic process triggered by Cd in bronchial epithelial cells.

Collectively, this study provides valuable new insights into the functional significance of circRNA-lncRNA-miRNA regulatory networks in Cd-induced malignant transformation, highlighting potential novel targets for future therapeutic interventions against lung cancer associated with cadmium exposure.

5 | Conclusion

In conclusion, this study identified a novel regulatory network involving circ_000877, lnc237177, miR-3192-5p, and CCND1/MMP-2 that promotes Cd-induced malignant transformation of 16HBE cells. Upregulated circ_000877 and lnc237177 co-targeted and negatively regulated miR-3192-5p, leading to increased expression of CCND1 and MMP-2, which ultimately facilitated the Cd-induced malignant transformation of human bronchial epithelial cells.

Ethics Statement

The manuscript does not contain clinical studies or patient data.

Conflicts of Interest

The authors declare no conflicts of interest.

Data Availability Statement

The data that support the findings of this study are available from the corresponding author upon reasonable request.

References

Chen, L., S. Li, W. Shi, and Y. Wu. 2022. "An Integrative Transcriptomic Analysis Reveals EGFR Exon-19 E746-A750 Fragment Deletion Regulated miRNA, circRNA, mRNA and lncRNA Networks in Lung Carcinoma." *International Journal of General Medicine* 15: 6031–6042.

Cui, Y., X. Wu, J. Jin, et al. 2023. "CircHERC1 Promotes Non-Small Cell Lung Cancer Cell Progression by Sequestering FOXO1 in the Cytoplasm and Regulating the miR-142-3p-HMGB1 Axis." *Molecular Cancer* 22, no. 1: 179.

Hu, J., H. Huang, Z. Xi, et al. 2022. "LncRNA SEMA3B-AS1 Inhibits Breast Cancer Progression by Targeting miR-3940/KLLN Axis." *Cell Death & Disease* 13, no. 9: 800.

Jiang, A., L. Gong, H. Ding, and M. Wang. 2021. "Cancer Mortality and Long-Term Environmental Exposure of Cadmium in Contaminated Community Based on a Third Retrospective Cause of Death Investigation of Residents Living in the Guangdong Province From 2004 to 2005." *Biological Trace Element Research* 199, no. 12: 4504–4515.

Kwon, Y., S. J. Park, B. T. Nguyen, et al. 2021. "Multi-Layered Proteogenomic Analysis Unravels Cancer Metastasis Directed by MMP-2 and Focal Adhesion Kinase Signaling." *Scientific Reports* 11, no. 1: 17130.

Li, C., Z. Wang, J. Zhang, et al. 2019. "Crosstalk of mRNA, miRNA, lncRNA, and circRNA and Their Regulatory Pattern in Pulmonary Fibrosis." *Molecular Therapy Nucleic Acids* 18: 204–218.

Li, X., Y. Jia, A. Nan, et al. 2019. "CircRNA104250 and lncRNAuc001dgp.1 Promote the PM2.5-Induced Inflammatory Response by Co-Targeting miR-3607-5p in BEAS-2B Cells." *Environmental Pollution* 258: 113749.

Liu, C., H. J. Li, W. X. Duan, et al. 2023. "MCU Upregulation Overactivates Mitophagy by Promoting VDAC1 Dimerization and Ubiquitination in the Hepatotoxicity of Cadmium." *Advanced Science (Weinh)* 10, no. 7: e2203869.

Liu, L., M. Gu, J. Ma, et al. 2022. "CircGPR137B/miR-4739/FTO Feedback Loop Suppresses Tumorigenesis and Metastasis of Hepatocellular Carcinoma." *Molecular Cancer* 21, no. 1: 149.

Lu, L., H. Qi, F. Luo, et al. 2017. "Feedback Circuitry via let-7c Between lncRNA CCAT1 and c-Myc Is Involved in Cigarette Smoke Extract-Induced Malignant Transformation of HBE Cells." *Oncotarget* 8, no. 12: 19285–19297.

McGraw, K. E., K. Schilling, R. A. Glabonjat, et al. 2024. "Urinary Metal Levels and Coronary Artery Calcification: Longitudinal Evidence in the Multi-Ethnic Study of Atherosclerosis." *Journal of the American College of Cardiology* 84, no. 16: 1545–1557.

Pietrzak, S., J. Wójcik, P. Baszuk, et al. 2021. "Influence of the Levels of Arsenic, Cadmium, Mercury and Lead on Overall Survival in Lung Cancer." *Biomolecules* 11, no. 8: 1160.

Sun, J., J. R. Hu, C. F. Liu, et al. 2023. "ANKRD49 Promotes the Metastasis of NSCLC via Activating JNK-ATF2/c-Jun-MMP-2/9 Axis." *BMC Cancer* 23, no. 1: 1108.

Valla, M., E. Klæstad, B. Ytterhus, and A. M. Bofin. 2022. "CCND1 Amplification in Breast Cancer—Associations With Proliferation, Histopathological Grade, Molecular Subtype and Prognosis." *Journal of Mammary Gland Biology and Neoplasia* 27, no. 1: 67–77.

Wang, D., S. Chen, Y. Shao, Y. Deng, and L. Huang. 2024. "EIF4A3 Modulated circ_000999 Promotes Epithelial-Mesenchymal Transition in Cadmium-Induced Malignant Transformation Through the miR-205-5p/ZEB1 Axis." *Environment International* 186: 108656.

Wang, G., L. Deng, K. Gong, P. Zhou, L. Peng, and C. Li. 2023. "Hsa_circ_0003528 Promotes Cell Malignant Transformation and Immune Escape via Increasing Oncogene PDL1 Through Sponging miR-511-3p in Non-Small Cell Lung Cancer." *Environmental Toxicology* 38, no. 6: 1347–1360.

Yan, Y., L. Jin, J. Li, and G. Chen. 2025. "Association of Cadmium and Lead Exposure With Mortality in Cancer Survivors: A Prospective Cohort Study." *Ecotoxicology and Environmental Safety* 292: 117960.

Yao, B., Q. Zhang, Z. Yang, et al. 2022. "CircEZH2/miR-133b/IGF2BP2 Aggravates Colorectal Cancer Progression via Enhancing the Stability of m6A-Modified CREB1 mRNA." *Molecular Cancer* 21, no. 1: 140.

Zhang, L., H. Tao, J. Li, E. Zhang, H. Liang, and B. Zhang. 2021. "Comprehensive Analysis of the Competing Endogenous circRNA-lncRNA-miRNA-mRNA Network and Identification of a Novel Potential Biomarker for Hepatocellular Carcinoma." *Aging* 13, no. 12: 15990–16008.

Zhu, W., H. Zhang, L. Tang, et al. 2024. "Identification of a Plasma Exosomal lncRNA- and circRNA-Based ceRNA Regulatory Network in Patients With Lung Adenocarcinoma." *Clinical Respiratory Journal* 18, no. 10: e70026.

Supporting Information

Additional supporting information can be found online in the Supporting Information section.